Fluorescent carbon-dots enhance light harvesting and photosynthesis by overexpressing *PsbP* and *PsiK* genes

Yuhui Wang[1†], Zhuomi Xie[2,3†], Xiuhua Wang[1], Xin Peng[2*] and Jianping Zheng[1*]

Abstract

Background: Fluorescent carbon-dots (CDs) with multifaceted advantages have provided hope for improvement of crop growth. Near infrared (NIR) CDs would be more competitive and promising than short-wavelength emissive CDs, which are not directly utilized by chloroplast. The molecular targets and underlying mechanism of these stimulative effects are rarely mentioned.

Results: NIR-CDs with good mono-dispersity and hydrophily were easily prepared by a one-step microwave-assisted carbonization manner, which showed obvious UV absorptive and far-red emissive properties. The chloroplast-CDs complexes could accelerate the electron transfer from photosystem II (PS II) to photosystem I (PS I). NIR-CDs exhibited a concentration-dependent promotion effect on *N. benthamiana* growth by strengthening photosynthesis. We firstly demonstrated that potential mechanisms behind the photosynthesis-stimulating activity might be related to up-regulated expression of the photosynthesis and chloroplast synthesis related genes, among which *PsbP* and *PsiK* genes are the key regulators.

Conclusion: These results illustrated that NIR-CDs showed great potential in the applications to increase crop yields through ultraviolet light harvesting and elevated photosynthesis efficiency. This work would provide a theoretical basis for the understanding and applications of the luminescent nanomaterials (not limited to CDs) in the sunlight conversion-related sustainable agriculture.

Keywords: Fluorescent carbon-dots, Photosynthesis, *N. benthamiana*, *PsbP*, *PsiK*

Background

Photosynthesis is one of the most fundamental biochemical processes of organisms, and it is vital to the plant growth on earth. Enhancing photosynthetic efficiency and electron transfer process are thought to be one of the efficient approaches for improving plant growth

[1]. Many strategies such as gene regulation [2], genetic improvement [3] and environmental modelling [4] have been applied to improve the photosynthetic efficiency in crops. In the photosynthesis process, sunlight utilization by chloroplasts of plants is limited to visible spectral range [5]. Therefore, it is very promising to build an artificial hybrid photosynthesis system to improve the ability of plants to capture and convert solar energy efficiently [6].

Luminescent nanomaterials (LNMs) have been paid more attention in many fields like chemo/biosensing, bioimaging, catalysis and nanomedicine due to their unique photophysical properties [7]. As light conversion agents, LNMs would have the potential to enhance sunlight

*Correspondence: pengx@nit.zju.edu.cn; zhengjianping@nimte.ac.cn
[†]Yuhui Wang and Zhuomi Xie have contributed equally to this work
[1] Cixi Institute of Biomedical Engineering, Ningbo Institute of Materials Technology and Engineering, Chinese Academy of Sciences, Ningbo 315300, People's Republic of China
[2] Ningbo Research Institute of Zhejiang University, Ningbo 315100, People's Republic of China
Full list of author information is available at the end of the article

Wang *et al. J Nanobiotechnol*   (2021) 19:260

Page 2 of 14

harvesting and promote photosynthesis efficiency [8]. In previous reports, semiconductor quantum dots (SQDs) [9], silicon quantum dots [10], lanthanide-doped up-conversion phosphors [11] and noble metal nanoclusters [12] were exploited on the plant growth and development. However, toxicity of the heavy metal ions, high cost and low fluorescence quantum yield greatly limit their further applications [13, 14]. Therefore, it is meaningful and challenging to seek new LNMs with the features of low cost, good biocompatibility and outstanding optical properties [15].

Recently, fluorescent carbon-dots (CDs) emerging as a new class of inorganic phosphors have attracted increasing attention [16–19]. Due to their obvious merits of facile and cheap preparation, excellent fluorescence characters, CDs have demonstrated many promising applications such as chemo/biosensing, bioimaging, catalysis, and optoelectronic devices [20–24]. Specially, most of the reported CDs are no/low toxic and biocompatible, and have been demonstrated great potential in biological-relevant fields [25]. However, some CDs with positive charge reveal cyto and geno-toxicity in some degree [26]. The biosafety of the longtime exposure to CDs remains to be a challenging issue, and should be taken into consideration [27]. The development of CDs in photosynthesis has become a hot research topic [28–33]. For instance, Chandra et al. reported a blue-emissive CDs-chloroplasts hybrid nanosystem to accelerate electron transfer from CDs to chloroplast [34]. Li et al. reported a strategy to enhance photosynthetic efficiency via light-harvesting with dual-emissive CDs [35]. Nonetheless, most of the CDs show short-wavelength blue/green emission, which is not directly utilized by chloroplast. To overcome the above issue, far-red emissive CDs with high quantum yield and good water-solubility were synthesized, and have demonstrated to be efficient in the enhancement of plant growth and photosynthesis [36]. Meanwhile, former researches have presented that CDs were no phytotoxicity on the growth of plants, and could be transferred from the roots to the stems and leaves through the vascular system [37]. The above reports confirmed that CDs would be competitive and promising agents to enhance photosynthesis or improve growth of crops. Nonetheless, the underlying mechanisms of these stimulative effects were hardly mentioned. There are few reports about the influence of CDs on the expression level of genes and the plant quality. [8]
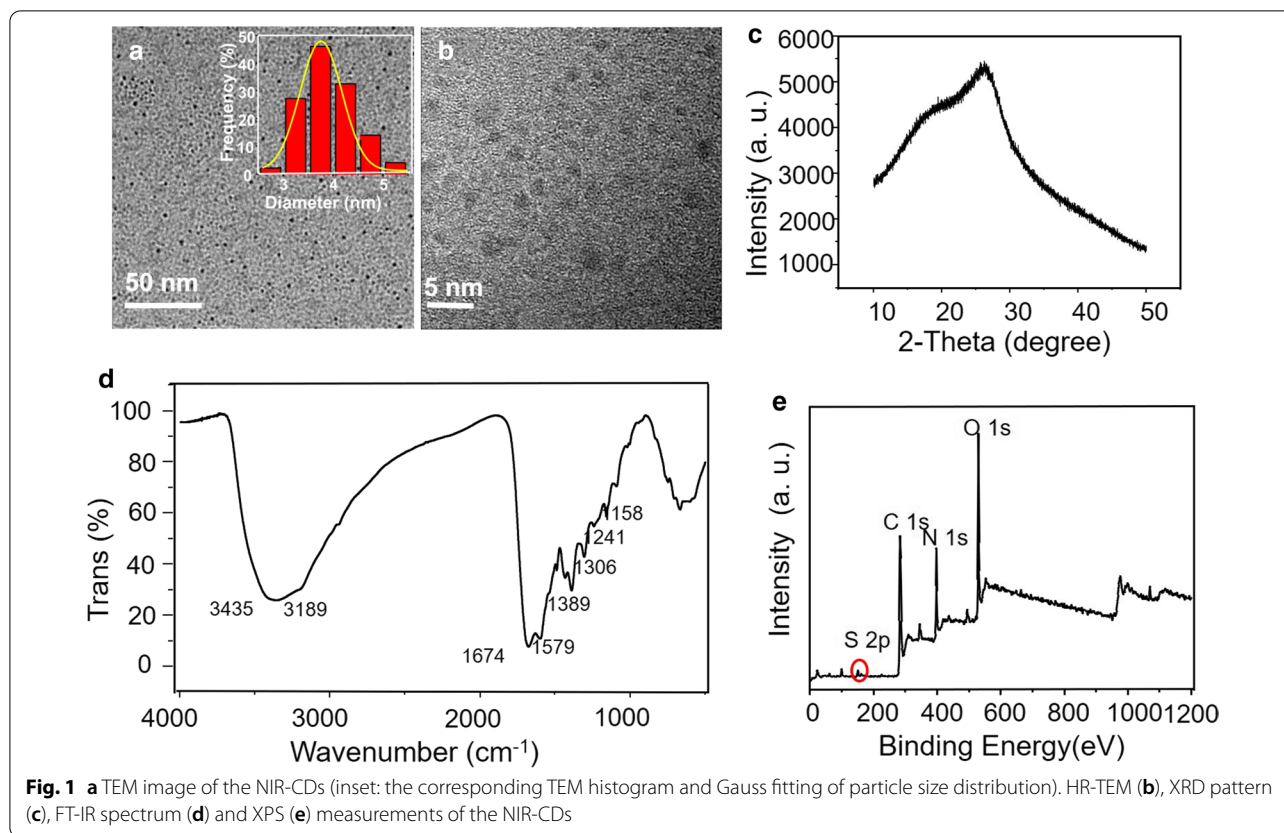
Herein, in order to understand the mechanism of CDs-caused enhancive photosynthesis efficiency, representative near-infrared (NIR) emissive CDs (a model light-conversion phosphors) and *Nicotiana* benthamiana (*N. benthamiana*, taken as a plant model) were preferentially selected, respectively. The NIR-CDs were verified to be effective in the enhancement of ultraviolet light absorption and the electron transfer from CDs to the chloroplasts *N. benthamiana*. So, improved photosynthetic efficiency was observed both in vivo and in vitro. Furthermore, some photosynthetic and chloroplast synthesis-relevant genes were inspected. The results demonstrated that *PsbP* and *PsiK* genes were the key regulators of the photosynthesis-stimulating effect that activated by the NIR-CDs. To the best of our knowledge, this is the first mechanism research on the genes level, which provides a manner to study the mechanism of LNMs-induced enhanced sunlight absorption and photosynthesis efficiency. In addition, this work would provide a theoretical basis for the understanding and applications of other luminescent nanomaterials (not limited to CDs) in the sunlight conversion-related sustainable agriculture.
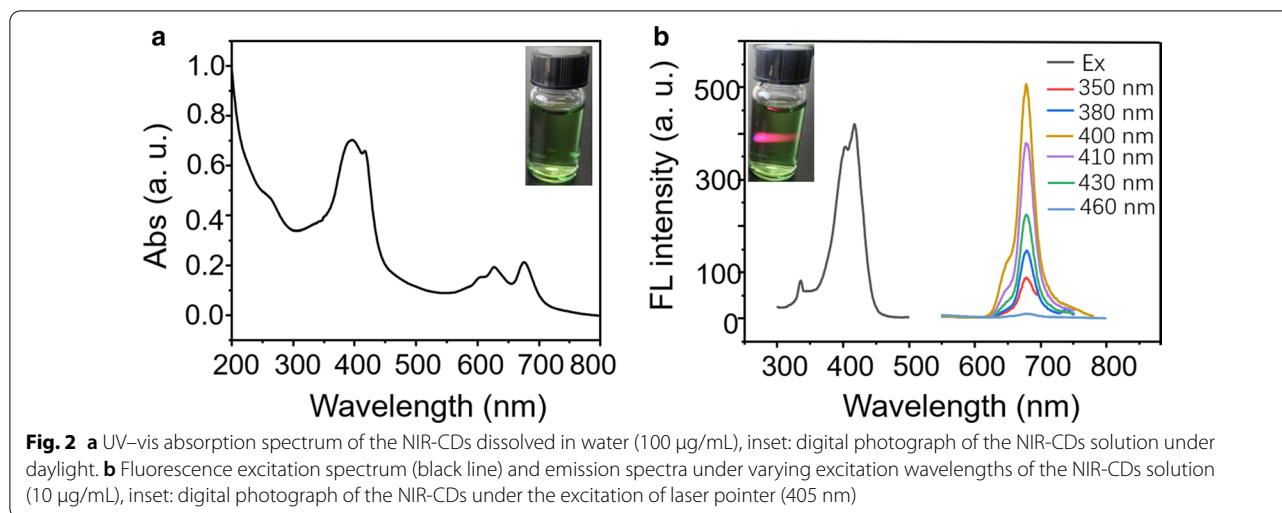
Results

Characterizations of the CDs

The NIR-CDs were facilely synthesized by a microwave-assisted carbonization method using glutathione and formamide as the raw materials. To characterize the morphology, structure and surface state of the prepared CDs, TEM, XRD, FT-IR, XPS, Raman and Zeta potential measurements were performed. As shown in Fig. 1a, the harvested NIR-CDs exhibit uniform and spherical morphologies with narrow size distribution and an average diameter of 3.8 nm. However, no obvious lattice fringes are observed in the HR-TEM image (Fig. 1b), implying that they are mostly noncrystalline. A typical peak at 26° [(002) plane] in the XRD pattern (Fig. 1c) further verifies the noncrystalline graphite structure of the CDs [38]. Typical Raman spectrum (Additional file 1: Figure S1) also confirms the graphite nature of the NIR-CDs. The distinct peaks at 1557 and 1321 cm^{-1} represent the typical G-band and D-band, respectively. Meanwhile, a low ratio of D to G strongly attests the existence of pristine carbon in the NIR-CDs [39]. In Fig. 1d, a broad and strong absorption band from 3000 to 3700 cm^{-1} with two peaks centered at 3435 and 3189 cm^{-1} is clearly observed, which is attributed to the stretching vibrations of O–H and N–H, demonstrating the existence and abundance of hydrophilic hydroxyl and amino groups. The peaks at 1674, 1579, 1389 cm^{-1} belong to the stretching vibrations of the C=O, C=C/C=N, and C–N bonds, respectively. The peaks at 1158 and 1241 cm^{-1} are attributed to C–O and C–N stretching vibrations. The absorption band at 1000–1100 cm^{-1} is attributed to C=S and oxidized S bonds [40, 41]. These FT-IR assignments are clearly verified by XPS analysis (Fig. 1e). Representative peaks of C 1 s, N 1 s, O 1 s, and S 2p are observed at 283, 397, 529, 161 eV, respectively, which indicates that the CDs mainly contain C, N, O and S elements (atom

Wang *et al. J Nanobiotechnol*   (2021) 19:260

Page 3 of 14

Fig. 1 **a** TEM image of the NIR-CDs (inset: the corresponding TEM histogram and Gauss fitting of particle size distribution). HR-TEM (**b**), XRD pattern (**c**), FT-IR spectrum (**d**) and XPS (**e**) measurements of the NIR-CDs

ration, C:O:N:S = 63.61:16.77:19.28:0.34). High resolution C 1 s spectrum (Additional file 1: Figure S2a) shows five peaks at 284.8, 286.3, 288, 289.4 and 291.2 eV, corresponding to C=C/C−C, C−N, C−O, C=N/C=O, and N−C=O, respectively. Three unique peaks of pyridine-like N, amino N, and pyrrolelike N at 398.6, 400.1, and 402.5 eV are observed in high resolution N 1 s spectrum (Additional file 1: Figure S2b). O 1 s XPS spectrum exhibit the typical peaks of C−OH and C=O at 531.5 and 533.7 eV, respectively (Additional file 1: Figure S2c). In addition, the higher solution S 2p spectrum (Additional file 1: Figure S2d) can be fitted with four binding energies of 162.2, 163.6, 164.7 and 168.7, which are assigned to thiolate, $2p_{3/2}$ and $2p_{1/2}$ of thiophene S, and oxidized S, respectively [42, 43]. Zeta potential measurement reveals that the NIR-CDs are negatively charged (ζ = − 15.8 mV, Additional file 1: Figure S3), which would enable strong electrostatic exclusion and colloid stability.

Next, the photophysical properties of the NIR-CDs were investigated in detail. Figure 2a represents the UV–Vis absorption spectrum. The NIR-CDs present three main absorption bands i.e., 240–300 nm, 350–450 nm, and 550–750 nm, which are generally assigned to the typical $\pi \rightarrow \pi^*$ transition of the aromatic C=C bond, $\pi \rightarrow \pi^*$ and $n \rightarrow \pi^*$ transitions of the aromatic π system

containing the C=O, C=N, and C=S bonds, respectively [44]. As shown in Fig. 2b, the CDs display brightly deep-red emission from 625 to 710 nm with a sharp peak centered at 680 nm. And an excitation-independent fluorescence emission property of the NIR-CDs is observed distinctly. The fluorescence excitation spectrum indicates that the excitation focuses on blue spectrum range with the optimal excitation wavelength of 420 nm. Moreover, the averaged lifetime is measured and calculated to be 2.8 ns with bi-exponential decays (Additional file 1: Figure S4), and the absolute fluorescence quantum yield of the NIR-CDs is measured to be 17.8% under the optimal excitation i.e., 420 nm. In addition, photostability of the NIR-CDs was estimated. In Additional file 1: Figure S5, the emission intensities slightly decrease upon the irradiation of ultraviolet lamp, implying good tolerance to photobleaching of the NIR-CDs. The CDs solution keeps very stable fluorescence emission even after one month storage at ambient environment (Additional file 1: Figure S6). So, the above unique optical properties e.g., strong absorption in the ultraviolet-blue region, efficient and stable emission in far-red region make this NIR-CDs promising agent in light-harvesting and electron transfer from photosystem II (PS II) to photosystem I (PS I) in chloroplasts.

Fig. 2 a UV–vis absorption spectrum of the NIR-CDs dissolved in water (100 μg/mL), inset: digital photograph of the NIR-CDs solution under daylight. **b** Fluorescence excitation spectrum (black line) and emission spectra under varying excitation wavelengths of the NIR-CDs solution (10 μg/mL), inset: digital photograph of the NIR-CDs under the excitation of laser pointer (405 nm)

NIR-CDs treatment significantly promoted the growth and development of *N. benthamiana*

N. benthamiana were cultured with different concentrations of NIR-CDs solution (experiment group) and pure water (control group), respectively. Figure 3 is the photograph of *N. benthamiana* exposed to different concentrations of NIR-CDs during 5 days. As shown in it, there is an obvious difference of growth vigour of *N. benthamiana* between the control group and CDs-treated groups. A concentration-dependent promotion effect on *N. benthamiana* growth was found in the concentration range of NIR-CDs from 0 to 0.1 mg/mL. It turned out that a concentration threshold (0.3 mg/mL) was presented, above which the differences were not significant. 0.05 mg/mL of the CDs was the optimum concentration.
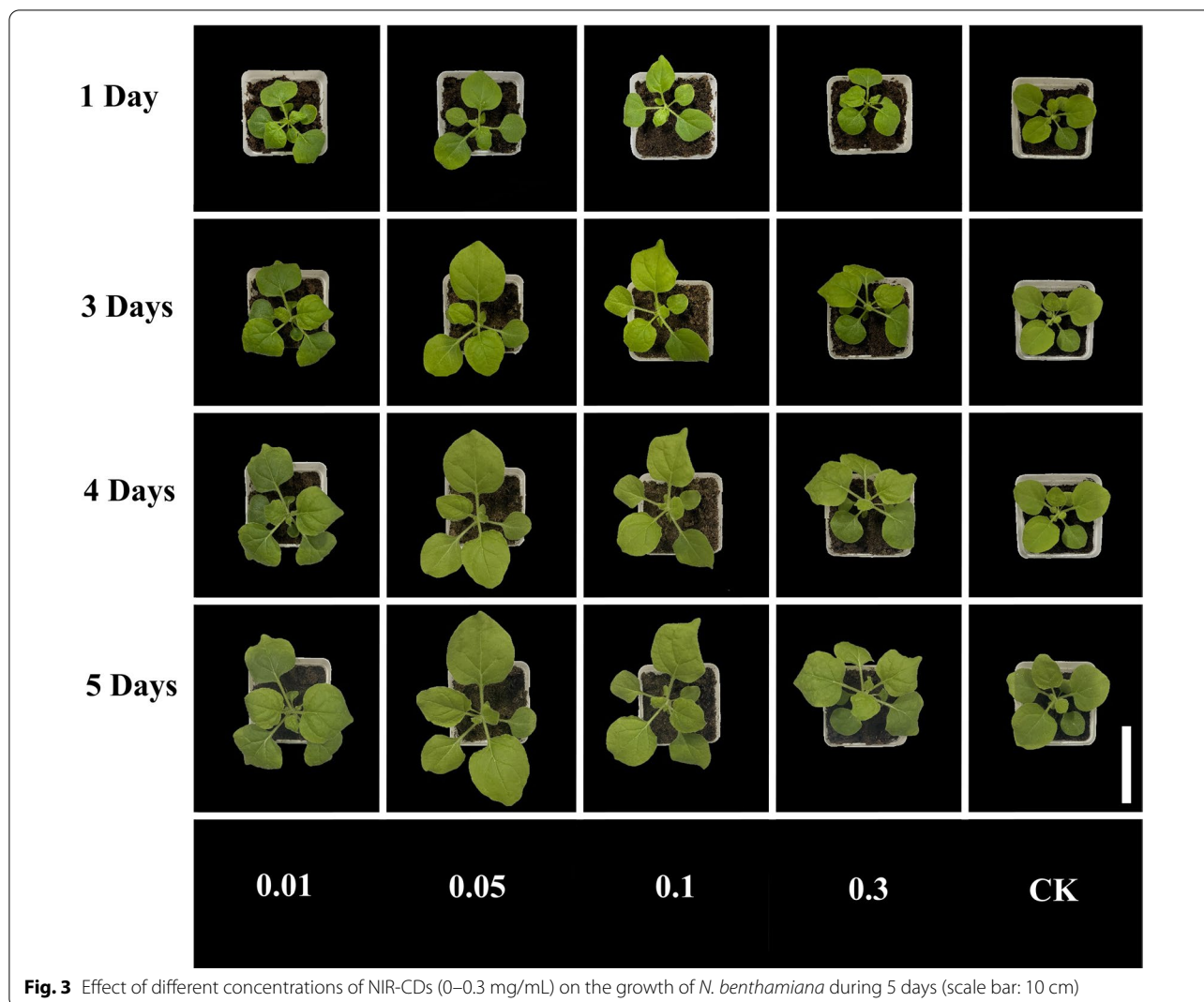
In order to obtain accurate results, root length, stem length, leaf area and biomass were measured at least three times, respectively. As shown in Fig. 4, it could be found that both the stem and root elongation depended on the concentration of NIR-CDs. The stem length of *N. benthamiana* exposed to the CDs (0.01 mg/mL, 0.05 mg/mL, 0.1 mg/mL and 0.3 mg/mL) was longer $44.83 \pm 3.9\%$, $143.1 \pm 9.8\%$, $32.76 \pm 4.1\%$ and $37.93 \pm 3.7\%$ than the control, respectively. As for the elongation of root length, they were $26.28 \pm 3.4\%$, $62.37 \pm 6.8\%$, $38.14 \pm 4.5\%$ and $32.98 \pm 4.3\%$, respectively. The leaf area exposed to CDs (0.01 mg/mL, 0.05 mg/mL, 0.1 mg/mL and 0.3 mg/mL) was increased by $14.54 \pm 2.2\%$, $57.27 \pm 4.6\%$, $29.94 \pm 2.5\%$, and $12.72 \pm 0.9\%$ than the control, respectively. When the concentration was 0.3 mg/mL, NIR-CDs didn't stimulate the growth of *N. benthamiana* anymore. 0.05 mg/mL of CDs improved root length, stem length and biomass prominently, which was the optimal concentration

for the growth of *N. benthamiana*, with a growth rate of single plant fresh weight of $247.03 \pm 26\%$. To further evaluate the metabolic activity of *N. benthamiana* under the treatment of different concentrations of NIR-CDs, the SOD activity was also investigated with the results shown in Fig. 4e. CDs at 0.01 mg/mL, 0.05 mg/mL, 0.1 mg/mL, and 0.3 mg/mL significantly increased SOD activity by $5.88 \pm 0.6\%$, $58.82 \pm 5.9\%$, $23.52 \pm 3.2\%$ and $29.41 \pm 3.2\%$ respectively, as compared to the control group.

Process of uptake and transmission of NIR-CDs in *N. benthamiana*

In order to study the uptake and translocation conditions of NIR-CDs in *N. benthamiana* during the growth stage, confocal images of root, stem, and leaf were displayed using Laser-scanning confocal fluorescence microscope after 5 days incubation with 0.05 mg/mL CDs. As shown in Fig. 5, the uptake of NIR-CDs by *N. benthamiana* could be identified in vivo due to the red luminescent emissions from CDs observed under 514 nm excitation. The bright field images were also investigated and overlain with luminescence images. In contrast, no red luminescence and any autofluorescence background of tissue were detected in the control group. The distribution of luminescence signals of CDs predominantly existed in the roots, and less in stems and leaves, revealing that CDs were absorbed by root and transported to the stems and leaves.

The confocal images also revealed that the CDs could penetrate cell wall into vascular bundle system. Thus, the growth-promoting effect of CDs might be due to the entry of CDs into plant cells to regulate plant physiological activities.
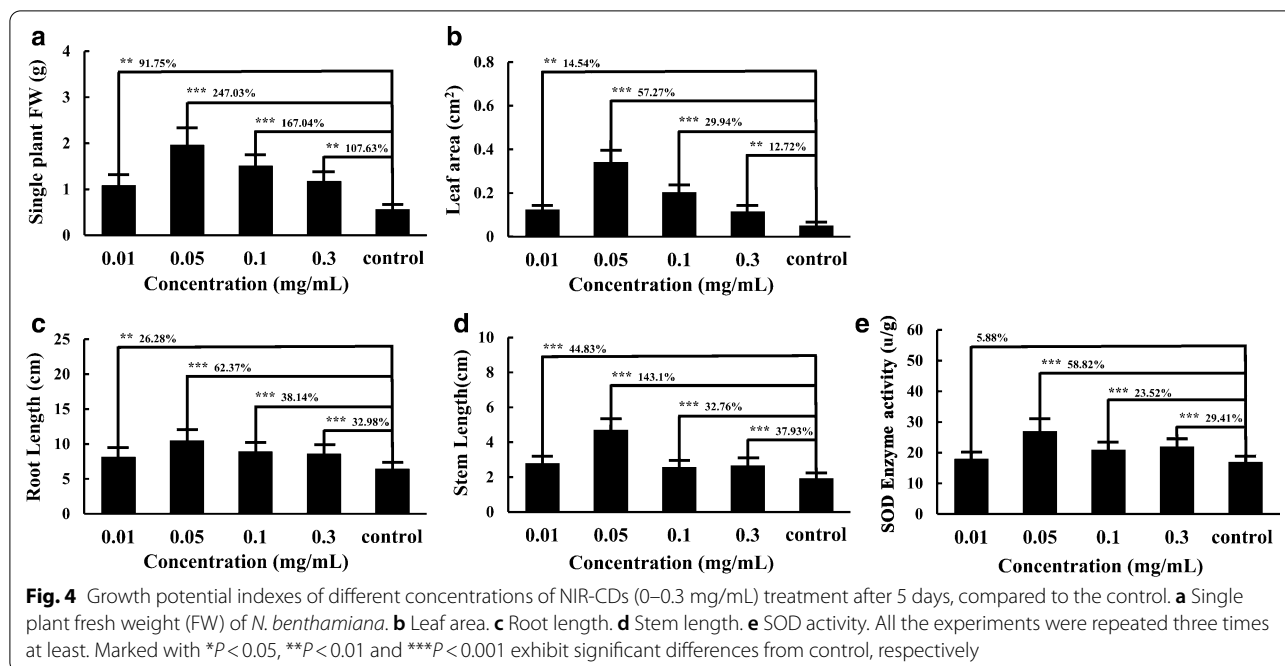
Wang *et al. J Nanobiotechnol*   (2021) 19:260

Page 5 of 14

Fig. 3 Effect of different concentrations of NIR-CDs (0–0.3 mg/mL) on the growth of *N. benthamiana* during 5 days (scale bar: 10 cm)

NIR-CDs treatment significantly improved chlorophyll content and photosynthesis

The effect of NIR-CDs treatment on photosynthesis was determined. 0.05 mg/mL of NIR-CDs enhanced chlorophyll content by 11.4%, 6.08%, and 10.21% in seven-leaf, ten-leaf, and thirteen-leaf stage, respectively ($P < 0.05$). CDs treatment induced significant increase in net photosynthetic rate at all the three stages, and the maximum increase (66.68%) was achieved by 0.05 mg/mL of CDs in thirteen-leaf stage. The rate of photosynthesis, which is evaluated by CO_2 entry through the stomata and fixation within the chloroplast, can change when plants are subjected to various treatments. Exposure to CDs at 0.05 mg/mL significantly increased the transpiration rate by 0.15–1.47%, stomatal conductance by 17.5–110.8% ($P < 0.01$) and intercellular CO_2 by 20.38–33.82% ($P < 0.01$) as compared to the control group (Fig. 6).

Growth-promoting effect of NIR-CDs were achieved by upregulating expression level of the genes involved in photosynthesis

The increased growth rate might be due to NIR-CDs stimulating the photosynthesis of *N. benthamiana* seedlings. To prove the conjecture, we investigated the effects of NIR-CDs on the gene expression level, which were involved in photosynthesis. In this work, eight major photosynthetic genes (*Psi-K*, *PsbP*, *PsbS1*, *PsbY*, *HCF136*, *PsbQ1*, *PsbQ2*, and *PsbO4*) of *N. benthamiana* were examined after 5 days incubation with 0.05 mg/mL NIR-CDs. The primers of these candidate genes and reference gene are displayed in Table 1. The results shown in Fig. 7 indicated that the CDs could activate significantly the overexpression of seven *N. benthamiana* photosynthetic genes compared with control group. Furthermore, the expression levels of *PsbP* and *Psi-K* genes were increased the most by 48-fold and 32-fold as compared

Wang *et al. J Nanobiotechnol* (2021) 19:260

Page 6 of 14

Fig. 4 Growth potential indexes of different concentrations of NIR-CDs (0–0.3 mg/mL) treatment after 5 days, compared to the control. **a** Single plant fresh weight (FW) of *N. benthamiana*. **b** Leaf area. **c** Root length. **d** Stem length. **e** SOD activity. All the experiments were repeated three times at least. Marked with *$P < 0.05$, **$P < 0.01$ and ***$P < 0.001$ exhibit significant differences from control, respectively

to the control, respectively. It revealed that *PsbP* and *Psi-K* genes were most sensitive to the stimulation effect of NIR-CDs. At the concentration of 0.05 mg/mL NIR-CDs, the expression levels of the five genes (*PsbS1*, *PsbY*, *PsbQ1*, *PsbQ2*, and *PsbO4*) were significantly increased by 148.3%, 246.7%, 90.3%, 98.4%, and 294.4%, respectively after incubation of 5 days. In addition, there were no significant differences in the expression level of *HCF136*, which suggested NIR-CDs had no significant effects on *HCF* family genes. These results coincided with the response of the chlorophyll content and photosynthetic rate.

Discussion

Enhanced sunlight harvesting and photosynthesis efficiency of the CDs- chloroplast hybrids in vitro

Generally, far-red radiation can promote the growth of plant [45]. Herein, in order to verify the NIR-CDs-induced enhanced photosynthesis, interaction between the CDs and chloroplast, and the classical Hill reaction were severally studied. In Fig. 8a, the isolated chloroplast suspension shows two obvious absorption bands i.e., 400–500 and 650–700 nm. But, after being covered with the CDs, the absorption of chloroplast-CDs complexes is broadened and enhanced remarkably, especially in UV region (350–400 nm), which is mainly attributed to the typical UV absorption property of NIR-CDs (Fig. 2a). So, the hybrid chloroplast-CDs photosystem would be much more efficient in the harvesting of solar light. As shown in Fig. 8b, fluorescence emissions of the CDs gradually

decrease along with the constant addition of chloroplast, implying relatively strong adsorption between each other. Considering good spectrum overlap (650–700 nm) between fluorescence emission of the NIR-CDs and absorption of chloroplast, we speculate that the reason for the above fluorescence quenching is the occurrence of energy transfer from the CDs to chloroplast [36, 46].

As mentioned above, the NIR-CDs possess an obvious UV absorption feature, and their fluorescence emissions overlap well with the absorption of chloroplasts in the far-red region. So, it is possible and desirable that the NIR-CDs can absorb and transform rarely-used UV radiation to highly utilized far-red light to enhance photosynthesis efficiency. To authenticate this hypothesis, a typical Hill reaction was performed. Hill reaction provide a facile method to research the light-dependent transfer of electrons by chloroplasts in photosynthesis that results in the cleavage of water molecules and liberation of oxygen [47, 48]. Owing to the strong capacity of electron capture, 2,6-dichlorophenolindophenol (DCPIP) is routinely used as an indicator to monitor the electrons transfer from PS II to PS I during the photoreaction process. The absorption alterations at 600 nm indicate the reduction of DCPIP. By this way, the photosynthesis rate was estimated through measuring the absorption change of DCPIP. In this study, a xenon lamp was adopted as the light source. As shown in Fig. 8c, upon the durative exposure, the absorption of DCPIP decreases obviously, suggesting the emergence of photosynthesis of the subjected chloroplasts. Compared with the isolated chloroplasts,
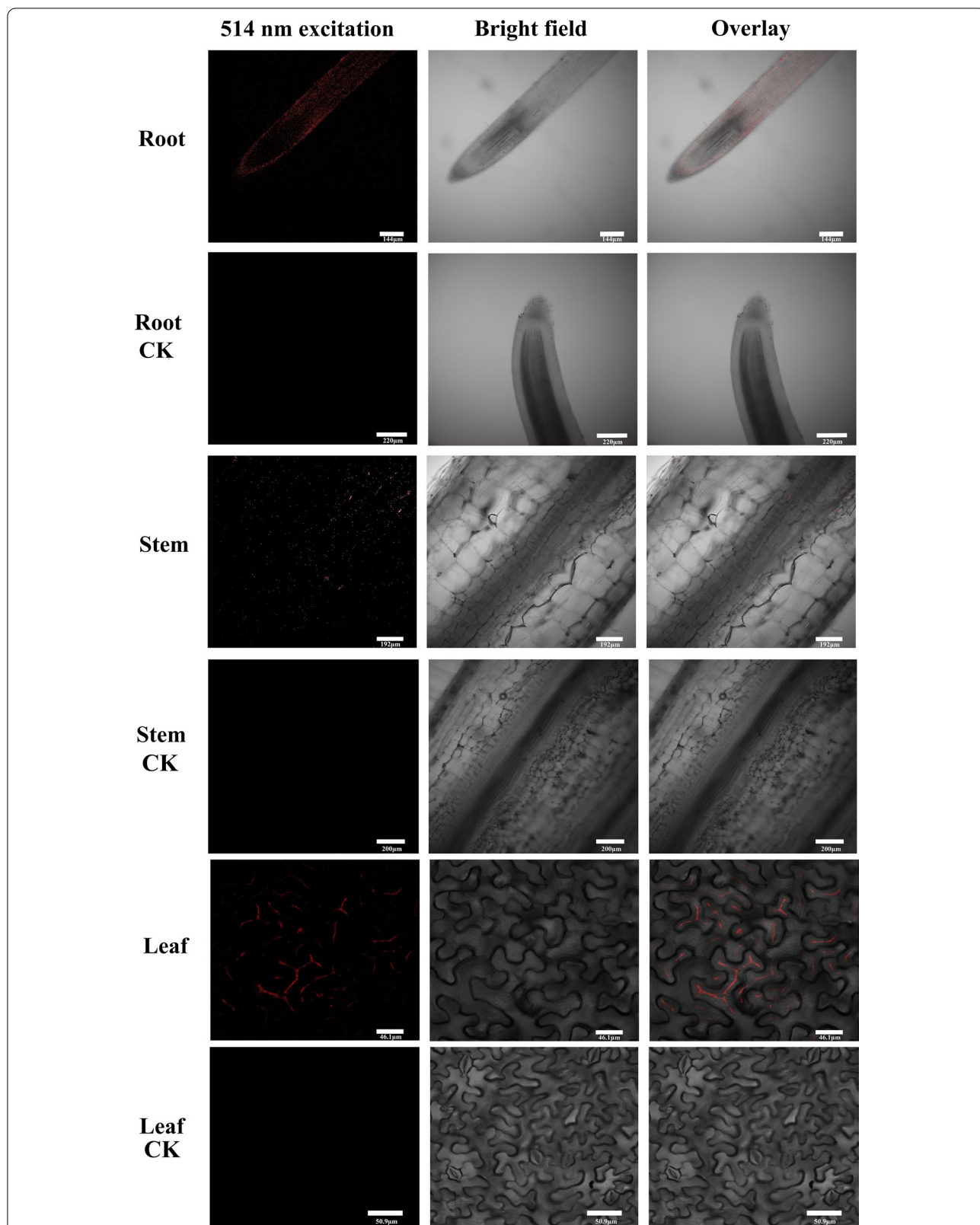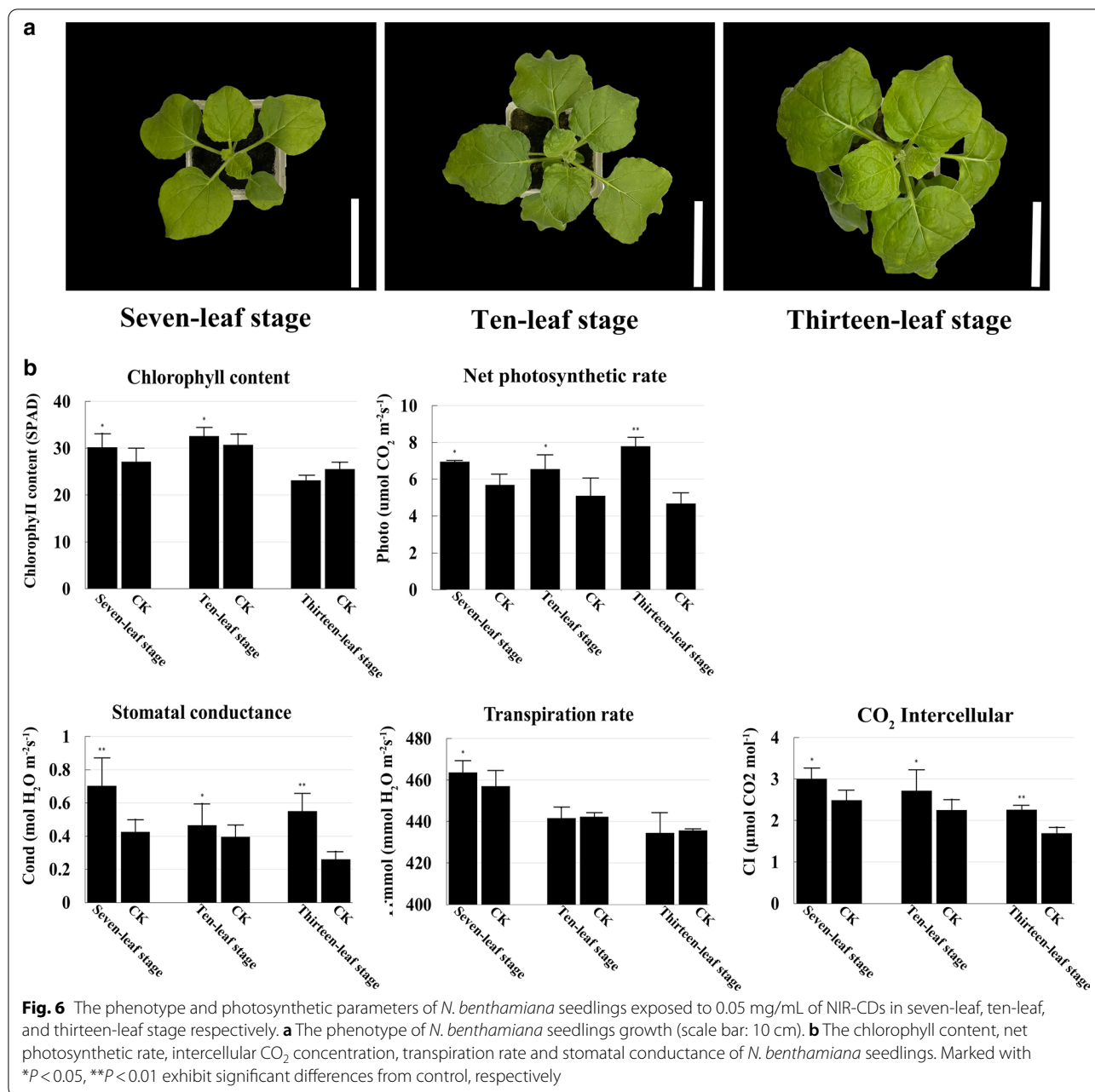
Wang *et al. J Nanobiotechnol*   (2021) 19:260

Page 7 of 14

Fig. 5 Laser scanning microscopy (LSM) images of root, stem, and leave cultured with NIR-CDs (0.05 mg/mL) for 5 days. All images were collected under the same exposure conditions

Wang *et al. J Nanobiotechnol*   (2021) 19:260

Page 8 of 14

Fig. 6 The phenotype and photosynthetic parameters of *N. benthamiana* seedlings exposed to 0.05 mg/mL of NIR-CDs in seven-leaf, ten-leaf, and thirteen-leaf stage respectively. **a** The phenotype of *N. benthamiana* seedlings growth (scale bar: 10 cm). **b** The chlorophyll content, net photosynthetic rate, intercellular CO_2 concentration, transpiration rate and stomatal conductance of *N. benthamiana* seedlings. Marked with *$P < 0.05$, **$P < 0.01$ exhibit significant differences from control, respectively

all the complexes of NIR-CDs-chloroplast can accelerate the reduction of DCPIP, and absorb and transform more UV light to far-red light that can be directly utilized by chloroplast. Thus, in the hybrid photosystem, the adoption of NIR-CDs is favorable for the light harvesting and utilization of chloroplasts in photosynthesis. Moreover, it is clearly to observe that the optimum concentration of the NIR-CDs is 50 μg/mL for the achievement of the highest photosynthesis rate. The above results obviously demonstrate that the proposed NIR-CDs show enhanced light harvesting in UV region, and their near infrared
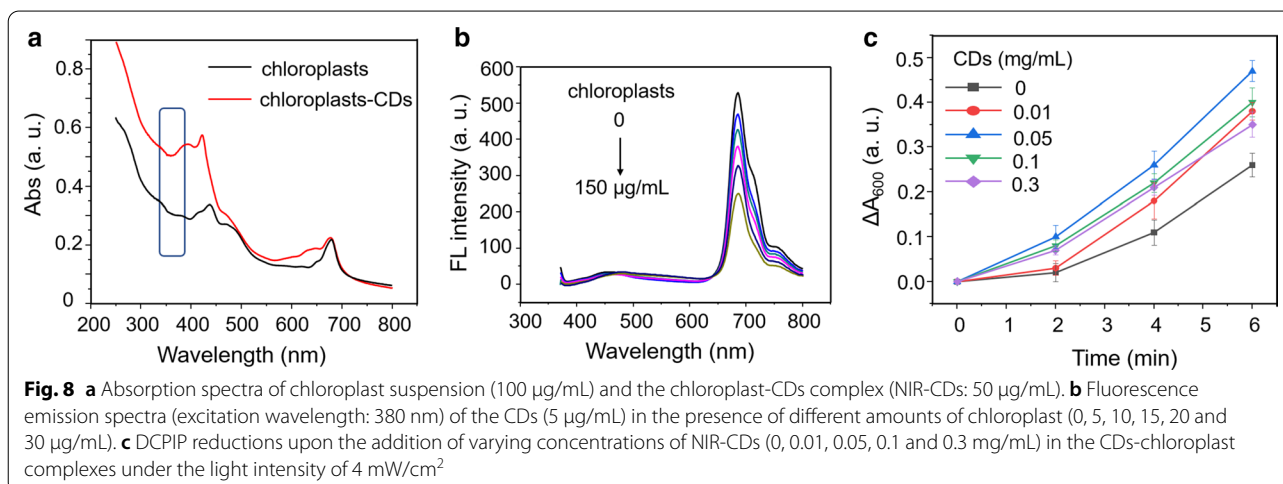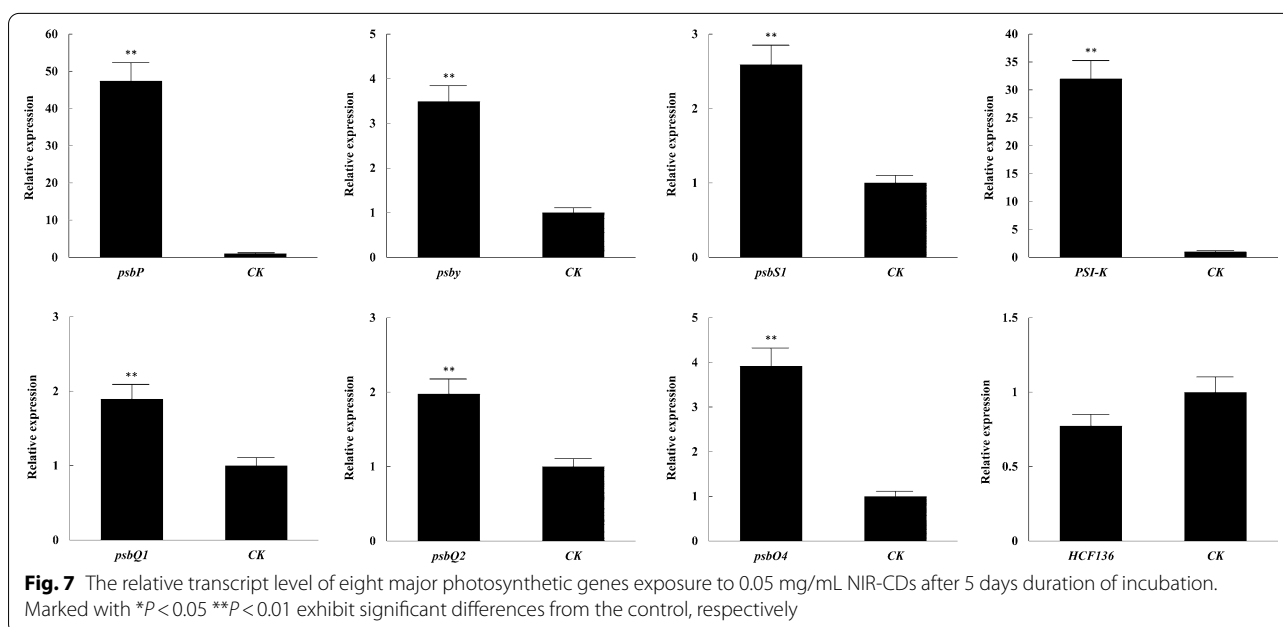
emissions would further promote the electrons transfer process from PS II to PS I, thereby improving the photosynthesis efficiency in vitro.

NIR-CDs strengthen photosynthesis by overexpressing PsbP and PsiK genes, promoting photosynthetic electron transfer and activating PSII and PSI in *N. benthamiana*

Photosynthesis is the key reaction to sustain life. In higher plants, oxygenic photosynthesis takes place in chloroplasts, in which protein complexes involved in the light-harvesting and photosynthetic electron transport

Wang *et al. J Nanobiotechnol* (2021) 19:260

Page 9 of 14

Table 1 Primer sequences of the genes involved in photosynthesis used for qRT-PCR analysis

Gene ID	Length (bp)	Primer-F (5′–3′)	Primer-R (5′–3′)
PsbP	138	GCTCTCACTGTCCTCATT	GAATCCATCTCCGTTGTATG
PsbS1	124	CTATGAAGCAGAGCCACTA	AGCCTTATCAAGACCAGTAG
Psi-K	121	CCATCAGCAAACAGGAAG	GACCAACAACACCACAAG
PsbQ1	129	TCGTCTCAGAGCAGAATAC	GCATGGTCCAGATCACTA
PsbQ2	112	ACCGTCATCTCTGCTAAG	GGCTGTTCTTGGTCTTTG
PsbO4	174	GTTCCTTGTGCCATCATAC	CTCAGCCGTGATCTTACCT
PsbY	153	GACATAGCAGAAGGAGACA	ACCAGTAAGACCAAGACC
HCF136	103	GCATTCTTATGTCGGCTAC	GTCACGAATCCATGTCTTG
GAPDH	125	AGCTCAAGGGAATTCTCGATG	AACCTTAACCATGTCATCTCCC

Fig. 7 The relative transcript level of eight major photosynthetic genes exposure to 0.05 mg/mL NIR-CDs after 5 days duration of incubation. Marked with *$P < 0.05$ **$P < 0.01$ exhibit significant differences from the control, respectively

Fig. 8 **a** Absorption spectra of chloroplast suspension (100 μg/mL) and the chloroplast-CDs complex (NIR-CDs: 50 μg/mL). **b** Fluorescence emission spectra (excitation wavelength: 380 nm) of the CDs (5 μg/mL) in the presence of different amounts of chloroplast (0, 5, 10, 15, 20 and 30 μg/mL). **c** DCPIP reductions upon the addition of varying concentrations of NIR-CDs (0, 0.01, 0.05, 0.1 and 0.3 mg/mL) in the CDs-chloroplast complexes under the light intensity of 4 mW/cm^2

Wang *et al. J Nanobiotechnol*   (2021) 19:260

Page 10 of 14

are located in thylakoid membranes. Two light-energy driven photosystems (PS), PSI and PSII, are key components of photosynthetic electron transport machinery [49].

Photosystem I (PSI) is a supramolecular complex consisting of 17 different polypeptides located in the higher plant membranes. PSI-K is a subunit of photosystem I, and is significant for organizing the peripheral light-harvesting complexes on the core antenna of PSI [50]. In the present study, the expression levels of *PsiK* gene were dramatically increased by 32-fold as compared to the control. The results suggested that *PsiK* also played a key role in response to the growth-promoting effect of NIR-CDs.

Molecular oxygen metabolism is vital for photosynthesis, which is generated mainly by photosystem II (PS II). Photosystem II (PSII) is a light-driven water–plastoquinone oxidoreductase, in which the oxygen-evolving complex (OEC) catalyzes the water-splitting reaction [51].

It is known that some membrane-extrinsic subunits associated to the lumenal side of PSII in higher plants, including *PsbO*, *PsbP*, *PsbQ*, and *PsbR*, play crucial roles in optimizing water-oxidizing activity [52]. Some studies about *PsbP*-lacking transgenic plants suggested that *PsbP* was essential for full PSII function and chloroplast development [53]. In *PsbP*-deficient *N. tabacum*, PSII was hypersensitive to light and rapidly inactivated when the repair process of damaged PSII was inhibited. Moreover, the manganese cluster of *PsbP*-deficient leaves was markedly unstable. Another study on *A. thaliana* where both *PsbQ* genes (psbQ-1 and psbQ-2) had been suppressed, demonstrated that *PsbQ* was indispensable for photoautotrophy under low-light stress [54]. Kakiuchi et al. confirmed that *PsbQ* could significantly compensate for functional defects of mutated *PsbPs*, suggesting that *PsbQ* had a role in stabilizing the functional binding of *PsbP* in higher plant PSII [51].

PsbP and *PsbQ* were shown to play different roles in PSII of plants, including the likelihood that *PsbP* was in closer association to the oxygen-evolving catalytic center, *PsbQ* might not be required for PSII assembly, but should be involved in stabilizing the binding of *PsbP* [49]. Suppression of *PsbP* might lead to a reduction in growth rate and a wide range of defects in PSII function, such as lower quantum yield, lower oxygen-evolving activity, and a slower electron transfer rate at the donor side of PSII [55]. However, the suppression of *PsbQ* did not result in the severe malfunction of PSII in *Arabidopsis* [54]. These results suggested that *PsbQ* might play a less important role in PSII of higher plant than *PsbP*.

Similar to these previous studies, in the present study, the expression levels of *PsbP* gene were increased the

most by 48-fold as compared to the control, and it was far higher than the expression levels of *PsbQ1* and *PsbQ2.* The results also indicated that *PsbP*, *PsbQ1,* and *PsbQ2* were the regulatory genes involved in PSII in response to the stimulation effect of NIR-CDs, especially *PsbP* was the dominant regulator for the growth-promoting effect of NIR-CDs.

A study on high chlorophyll fluorescence (*HCF*) photosynthetic mutants of Arabidopsis led to the identification of HCF136. It was a nucleus-encoded assembly factor, which was essential for assembly or stability of the PSII reaction center complex, and might function as a chaperone-like assembly factor. *HCF136* was also reported to be required for efficient repair of PSII in Synechocystis [56]. On the contrary, another *HCF136* homologue was reported to be needless for assembly of the PSII, and hence was not required for photoautotrophic growth of *Synechococcus* PCC 7002 [57]. In the present study, no significant changes in the expression level of *HCF136* gene were observed in response to the stimulating photosynthesis effect of NIR-CDs, which also indicated that *HCF136* was not closely associated with photoautotrophy of *N. benthamiana.*

Previously, far-red emissive CDs (FR-CDs) have been synthesized and applied for enhanced sunlight absorption and photosynthesis efficiency [36]. The as-prepared FR-CDs was an efficient converter transferring ultraviolet A (UV-A) light to 625−800 nm far-red emission, which could be directly absorbed and utilized by chloroplasts. The in vivo experiment demonstrated 51.14% enhancement of fresh weights compared with that of the control group. Compared with the FR-CDs, the proposed NIR-CDs showed similar absorption range, but relatively narrow emission band (625–720 nm). Due to the better spectrum overlap between the NIR-CDs emission and the absorption of chloroplast (640–710 nm), much more photons were absorbed and transferred to chloroplast, and thereby improving the photosynthesis [58]. Aa a result, the enhancement of fresh weight reached to 247.03%, nearly five times than that of FR-CDs-caused weight enhancement. Moreover, in this work, it is the first report on the mechanism research in the molecular level of genes. It would provide a manner to study the interaction mechanism between luminescent nanomaterials and photosynthesis-related genes. A detailed comparison on optical properties, fresh weight enhancement, toxicity and mechanism between this work and previous reports is summarized in Additional file 1: Table S1. As shown therein, the proposed NIR-CDs show overall advantages compared to the previous luminescent nanomaterials.

Conclusion

In summary, NIR emissive CDs were successfully adopted for enhanced photosynthesis both in vitro and in vivo, and the activation mechanism was further illustrated by gene analysis. The CDs with good mono-dispersity and hydrophily were easily prepared by a one-step microwave-assisted carbonization manner. The obtained NIR-CDs showed obvious absorption in the UV region, strong and stable far-red fluorescence emission. The hybridized chloroplast-CDs complexes revealed effective absorption in UV region and accelerated the electron transfer from photosystem II (PS II) to photosystem I (PS I). NIR-CDs exhibited a concentration-dependent promotion effect on *N. benthamiana* growth, and it was achieved by strengthening photosynthesis. Seven photosynthetic genes and chloroplast synthesis related genes were demonstrated to be closely related to the photosynthesis-stimulating effect, among which *PsbP* and *PsiK* genes were the key regulators. The results in this work revealed the underlying molecular responders in response to NIR-CDs treatment. This result could provide a theoretical basis for expanding the applications of nanomaterial in sustainable agriculture practices.

Materials and methods
Materials and apparatus

Reduced glutathione, Na_2HPO_4, KH_2PO_4 and KCl were obtained from Aladdin Chemistry Co., Ltd (Shanghai, China). Sucrose, formamide and 2,6-dichlorophenolindophenol (DCPIP) were purchased from Sinopharm Chemical Reagent Co., Ltd. (Shanghai, China). All reagents were used as received without further purification. All aqueous solutions were prepared using deionized (DI) water.

A microwave oven [Galanz, P70F20CL-DG(B0)] was employed for the synthesis of CDs. The sizes and morphologies of the CDs were characterized by high resolution transmission electron microscopy (HR-TEM) (Tecnai F20) with an acceleration voltage of 200 kV. Fourier transform infrared (FT-IR) spectrum was performed on a Nicolet 6700 FT-IR spectrometer via the KBr pellet method. X-ray photoelectron spectroscopy (XPS) measurements were performed on a ESCALAB 250Xi (Thermo Scientific). The crystal phase of NIR-CDs was identified by a Bruker D8 Discover X-ray diffractometer (XRD) with 2θ range from 10° to 50° at a scanning rate of 4°/min, with Cu Ka irradiation (k = 1.5406 Å). Raman spectrum was recorded on a Renishaw inVia Raman spectrophotometer using 532 nm laser as the excitation resource. Fluorescence excitation and emission spectra were recorded on a Perkin Elmer spectrophotometer (LS-55). UV–Vis absorption were obtained from a

Agilent Cary 300 spectrophotometer. Fluorescence lifetimes were measured by Fluorolog 3–11 (HORIBA Jobin Yvon). Absolute fluorescence quantum yield of the CDs was determined by a Fluoromax-4 measurement system (HORIBA, JobinYvon. Inc).

Preparation of NIR-CDs

The CDs were synthesized via a one-step microwave-assisted carbonization manner [36, 59]. In brief, reduced glutathione (0.5 g) was dissolved in 20 mL formamide under ultrasonic treatment for 5 min. Subsequently, the mixture was transferred into a domestic microwave oven (700 W) for 3 min. After being cooled down to room temperature naturally, the obtained dark green solution was centrifuged at 10,000 rpm for 5 min to remove large-sized nanoparticles, and purified by a dialysis of 5 days (cut-off molecular weight, 3500). Then, the CDs solution was dried by a rotary evaporation to remove water. Finally, the product i.e., dark green NIR-CDs powder was harvested.

Isolation of chloroplasts

Chloroplasts were extracted from fresh leaves of tobacco that planted in our lab. The procedures were performed according to the previous literature [38]. Briefly, 5 g fresh leaves were cleaned by water and cut into small pieces, and then transferred into sucrose buffer (0.4 M sucrose, 0.03 M Na_2HPO_4, 0.02 M KH_2PO_4 and 0.01 M KCl, pH 7.7). After a quick grind of 5 min, the filtrate was centrifuged at 1000 rpm for 3 min to remove large residues. And the supernatant was collected and centrifuged at 3000 rpm for 3 min. Finally, the precipitate was collected and re-dispersed in 5 mL sucrose buffer to obtain a chloroplast suspension with the concentration calculated to be ca. 2.0 mg/mL. All the operations were carried out in the dark at 0–4 ℃.

Fabrication of the CDs/chloroplast complex

To acquire the complex of CDs-chloroplast, a simple mix between NIR-CDs and chloroplast suspension was performed in the sucrose buffer for 0.5 h at 4 ℃. The CDs would interact with chloroplasts, and were adsorbed onto the surface of chloroplasts and then form the CDs/chloroplast complexes.

Plant cultivation and NIR-CDs treatment

Nicotiana benthamiana (*N. benthamiana*) seeds were germinated in dark and moist conditions for 3 days. The germinated seeds were transferred into planting cups and cultured in a greenhouse (25 ± 2 ℃, 60% relative humidity, 400 μmol/m/s light intensity, 16 h light/8 h dark photoperiod). Then, seedlings in six-leaf stage showing consistent growth were selected and uniformly

divided into five groups. NIR-CDs solutions at 0.01 mg/mL, 0.05 mg/mL, 0.1 mg/mL, 0.3 mg/mL were sprayed on seedlings with a dosage of 20 mL/pot on the second day after transplantation, and 20 ml of ultrapure water was sprayed as the control. Phenotypic changes were observed and recorded for the next 5 days. Each treatment was repeated three times with ten plants.

Growth potential index determination

The root length, stem length, leaf area and single plant fresh weight (FW) of 10 N. *benthamiana* seedlings from each concentration of NIR-CDs treatment were measured after 5 days. Fresh weight was determined by gravimetric method. Growth rate of single plant fresh weight was expressed as percent (%) = (single plant fresh weight of treatment group sample − single plant fresh weight of control group sample)/single plant fresh weight of control group sample × 100%. The top two leaves of 10 seedlings from each treatment were collected for the measurement of leaf area.

The activity of superoxide dismutase (SOD) was determined according to our previous report [40] by following the photo-reduction of nitroblue tetrazolium (NBT) at 560 nm.

Uptake and translocation of NIR-CDs visualized by laser confocal

Laser confocal images were obtained from *N. benthamiana* seedlings after 5 days of treatment to track the fluorescence of CDs. The complete part of the root tip, blade back of leaves without veins, and the transection of stem were selected for preparing seedling tissue sections by hand-slicing. Then the tissue sections were placed into clean glass slides, followed by covering with a cover slip for fixation. Subsequently, thin slices of different parts (root, stem and leaf) of the plants were observed by Leica laser scanning confocal microscopy (LEICA TCS SP8, GER) excited at 488−587 nm to identify the locations of NIR-CDs [50].

Photosynthetic efficiency and pigment measurement

N. benthamiana seedlings treated with 0.05 mg/mL of NIR-CDs solution were sampled and determined in seven-leaf, ten-leaf, and thirteen-leaf stage, respectively. Net photosynthetic rate (Pn), transpiration rate (Tr), stomatal conductance (Cond), and mesophyll intercellular CO_2 (Ci) were measured using LI-6400 portable photosynthesis meter (Li-COR company, USA) according to a reported method [40]. The total chlorophyll (Chl a + b) contents of *N. benthamiana* leaves were measured using SPAD (Special Products Analysis Division)-502® plus chlorophyll meter (Minolta Camera Co., Osaka, Japan).

Quantitative qPCR analysis of the genes involved in photosynthesis

Based on the above photosynthetic physiological indexes, NIR-CDs solutions at 0.05 mg/mL was the optimal treatment concentration. After a treatment of 5 days, the leaves of 0.05 mg/mL NIR-CDs treatment were frozen quickly with liquid nitrogen, and the seedlings sprayed with ultrapure water were used as control. The total RNA in these leaves was extracted and reverse-transcribed to cDNA using a Plant Total RNA Reagent (Invitrogen) and TransScript All-in-One First-Strand cDNA Synthesis SuperMix for qPCR (TransGen Biotech, Beijing, China) following the manufacturer's protocol, respectively. The genes expression levels of *PSI-K* (AY899937.1) in photosystem I, *psbP* (KF460578.1), *psbS1* (EU645483.1), *psbY* (EH369921.1), *HCF136* (EH364276.1) in photosystem II, and *psbQ1* (JF897611.1), *psbQ2* (JF89761 2.1), *psbO4* (JF897606.1) for precursors of chloroplasts synthesis were measured by quantitative real-time (qRT)-PCR analysis using *GAPDH* as an internal reference. The genes sequences were retrieved from National Center for Biotechnology Information (https://www.ncbi.nlm.nih.gov/) to design primers (Table 1) using Primer Premier software, version 5. Each reaction contained 1 μL of cDNA, 5 μL of 2 × Power SYBR green PCR master mix (Applied Biosystems, Forster City, CA, USA), and 1 μL of forward and reverse primers in a final volume of 10 μL. Finally, the relative gene expression level was calculated using the $2^{-\Delta\Delta CT}$ method. Dissociation-curve analysis was carried out to confirm the amplification specificity. Three technical replicates were performed for each sample.

Statistical analysis

All experiments results were expressed as means ± standard deviation (SD). Statistical significance of all data was determined using a one-way analysis of variance (ANOVA) and the significance between treatments was assessed by LSD multiple comparison test at $P < 0.05$.

Supplementary Information

Additional file 1: Figure S1. Raman spectrum of the NIR-CDs. **Figure S2.** High resolution XPS spectra of C 1 s (a), N 1 s (b), O 1 s (c) and S2p (d), respectively. **Figure S3.** Zeta potential measurement of the NIR-CDs. **Figure S4.** FL decay fitting curve of the NIR-CDs (10 μg/mL) in water (λ_{ex} = 420 nm, λ_{em} = 680 nm). **Figure S5.** Photostability measurement of the CDs (10 μg/mL, relative intensities recorded at 680 nm) under continuous UV-light irradiation. **Figure S6.** The storage stability assessment of the CDs (100 μg/mL) in aqueous solution. **Table S1.** A detailed comparison on optical properties, toxicity and mechanism between this work and previous reports.

Wang *et al. J Nanobiotechnol*   (2021) 19:260

Page 13 of 14

Availability of data and materials

The genes sequences of *N. benthamiana* were retrieved from National Center for Biotechnology Information (https://www.ncbi.nlm.nih.gov/). Complementary data of CDs are supplied as Additional file 1.

Declarations

Ethics approval and consent to participate

Not applicable.

Consent for publication

All Authors have agreed to submit it in its current form for consideration for publication in your journal.

Competing interests

There are no conflicts to declare.

Author details

[1]Cixi Institute of Biomedical Engineering, Ningbo Institute of Materials Technology and Engineering, Chinese Academy of Sciences, Ningbo 315300, People's Republic of China. [2]Ningbo Research Institute of Zhejiang University, Ningbo 315100, People's Republic of China. [3]Fujian Agriculture and Forestry University, Fuzhou 350028, People's Republic of China.

References

1. Oleńska E, Małek W, Wójcik M, Swiecicka I, Thijs S, Vangronsveld J. Beneficial features of plant growth-promoting rhizobacteria for improving plant growth and health in challenging conditions: a methodical review. Sci Total Environ. 2020;743: 140682.
2. Rodríguez H, Fraga R, Gonzalez T, Bashan Y. Genetics of phosphate solubilization and its potential applications for improving plant growth-promoting bacteria. Plant Soil. 2006;287:15.
3. Uga Y, Kitomi Y, Ishikawa S, Yano M. Genetic improvement for root growth angle to enhance crop production. Breeding Sci. 2015;65(2):111.
4. Mercedes R, Romero-Aranda MR, Jurado O, Cuartero J. Silicon alleviates the deleterious salt effect on tomato plant growth by improving plant water status. J Plant Physiol. 2006;163(8):847.
5. Mickens MA, Torralba M, Robinson SA, Spencer LE, Romeyn MW, Massa GD, Wheeler RM. Growth of red pak choi under red and blue, supplemented white, and artificial sunlight provided by LEDs. Sci Hortic. 2019;245:200.
6. Lin X, Li Y, Saravanakumar S, Tang Q, Zhang S, Gao X, Hu Y, Huang K, Han G. Sunlight-operable light converting smart windows for fertilizer-free plant growth enhancement. Nano Today. 2020;34: 100918.
7. Guo Z, Park S, Yoon J, Shin I. Recent progress in the development of near-infrared fluorescent probes for bioimaging applications. Chem Soc Rev. 2014;43:16.
8. Yu J, Yu H, Li L, Ni X, Song K, Wang L. Influence of luminescent nanomaterials on plant growth and development. ChemNanoMat. 2021;7:859.
9. Li X-B, Tung C-H, Wu L-Z. Semiconducting quantum dots for artificial photosynthesis. Nat Rev Chem. 2018;2:160.
10. Li Y, Li W, Zhang H, Liu Y, Ma L, Lei B. Amplified light harvesting for enhancing Italian lettuce photosynthesis using water soluble silicon quantum dots as artificial antennas. Nanoscale. 2020;12:155.
11. Dong R, Li Y, Li W, Zhang H, Liu Y, Ma L, Wang X, Lei B. Recent developments in luminescent nanoparticles for plant imaging and photosynthesis. J Rare Earth. 2019;37:903.
12. Gautam A, Gore PM, Kandasubramanian B. Nanocluster materials in photosynthetic machines. Chem Eng J. 2020;385: 123951.
13. Tsoi KM, Dai Q, Alman BA, Chan WCW. Are quantum dots toxic? Exploring the discrepancy between cell culture and animal studies. Acc Chem Res. 2013;46:662.
14. Li Q, Zeman CJ IV, Ma Z, Schatz GC, Gu XW. Bright NIR-II photoluminescence in rod-shaped icosahedral gold nanoclusters. Small. 2021;17: 2007992.
15. Gong Y, Zhao J. Small carbon quantum dots, large photosynthesis enhancement. J Agric Food Chem. 2018;66(35):9159.
16. Wang B, Song H, Qu X, Chang J, Yang B, Lu S. Carbon dots as a new class of nanomedicines: opportunities and challenges. Coord Chem Rev. 2021;442: 214010.
17. Zulfajri M, Abdelhamid HN, Sudewi S, Dayalan S, Rasool A, Habib A, Huang GG. Plant part-derived carbon dots for biosensing. Biosensors. 2020;10:68.
18. Abdelhamid HN, Talib A, Wu HF. One pot synthesis of gold-carbon dots nanocomposite and its application for cytosensing of metals for cancer cells. Talanta. 2017;166:357.
19. Abdelhamid HN, Wu HF. Polymer dots for quantifying the total hydrophobic pathogenic lysates in a single drop. Colloids Surf B Biointerfaces. 2014;115:51.
20. Wan J, Zhang X, Zhang K, Su Z. Biological nanoscale fluorescent probes: from structure and performance to bioimaging. Rev Anal Chem. 2020;39:209.
21. Goel S, Mishra P. Thymoquinone loaded mesoporous silica nanoparticles retard cell invasion and enhance in vitro cytotoxicity due to ROS mediated apoptosis in HeLa and MCF-7 cell lines. Mater Sci Engineer C. 2019;104: 109891.
22. Li K, Zhao X, Wei G, Su Z. Recent advances in the cancer bioimaging with graphene quantum dots. Curr Med Chem. 2018;25:2876.
23. Lim S, Shen W, Gao Z. Carbon quantum dots and their applications. Chem Soc Rev. 2015;44:362.
24. Zhang M, Cheng J, Hu J, Luo J, Zhang Y, Lu F, Kong H, Qu H, Zhao Y. Green Phellodendri Chinensis Cortex-based carbon dots for ameliorating imiquimod-induced psoriasis-like inflammation in mice. J Nanobiotechnol. 2021;19:105.
25. Wang W, Cheng L, Liu G. Biological applications of carbon dots. Sci China Chem. 2014;57:522.
26. Havrdova M, Hola K, Skopalik J, Tomankova K, Petr M, Cepe K, Polakova K, Tucek J, Bourlinos AB, Zboril R. Toxicity of carbon dots—effect of surface functionalization on the cell viability, reactive oxygen species generation and cell cycle. Carbon. 2016;99:238.
27. Chaudhary S, Umar A, Bhasin KK, Singh S. Applications of carbon dots in nanomedicine. J Biomed Nanobiotech. 2017;13:591.
28. Wang H, Zhang M, Song Y, Li H, Huang H, Shao M, Liu Y, Kang Z. Carbon dots promote the growth and photosynthesis of mung bean sprouts. Carbon. 2018;136:94.
29. Lia Y, Pan X, Xu K, Wu Y, Zhuang J, Zhang X, Zhang H, Lei B, Hu C, Liu Y. Carbon dots as light converter for plant photosynthesis: augmenting light coverage and quantum yield effect. J Hazardous Mater. 2021;410: 124534.
30. Budak E, Erdoğan D, Ünlü C. Enhanced fluorescence of photosynthetic pigments through conjugation with carbon quantum dots. Photosynth Res. 2021;147:1.
31. Li Y, Xu X, Wu Y, Zhuang J, Zhang X, Zhang H, Lei B, Hu C, Liu Y. A review on the effects of carbon dots in plant systems. Mater Chem Front. 2020;4:437.
32. Tan TL, Zulkifli NA, Zamana ASK, Jusoh MB, Yaapar MN, Rashid SA. Impact of photoluminescent carbon quantum dots on photosynthesis efficiency of rice and corn crops. Plant Physiol Biochem. 2021;162:737.
33. Chakravarty D, Erande MB, Late DJ. Graphene quantum dots as enhanced plant growth regulators: effects on coriander and garlic plants. J Sci Food Agric. 2015;95(13):2772.
34. Chandra S, Pradhan S, Mitra S, Patra P, Bhattacharya A, Pramanik P, Goswami A. High throughput electron transfer from carbon dots to chloroplast: a rationale of enhanced photosynthesis. Nanoscale. 2014;6:3647.

Wang *et al. J Nanobiotechnol*   (2021) 19:260

Page 14 of 14

35. Li W, Wu S, Zhang H, Zhang X, Zhuang J, Hu C, Liu Y, Lei B, Ma L, Wang X. Enhanced biological photosynthetic efficiency using light-harvesting engineering with dual-emissive carbon dots. Adv Funct Mater. 2018;28:1804004.

36. Li DN, Li W, Zhang HR, Zhang XJ, Zhuang JL, Liu YL, Hu CF, Lei BF. Far-Red carbon dots as efficient light-harvesting agent for enhanced photosynthesis. ACS Appl Mater Interfaces. 2020;12(18):21009.

37. Li W, Zheng YJ, Zhang HR, Liu ZL, Su W, Chen S, Liu YL, Zhuang JL, Lei BF. Phytotoxicity, uptake and translocation of fluorescent carbon dots in mung bean plants. ACS Appl Mater Interfaces. 2016;8(31):19939.

38. Nimi N, Ariya S, Shaiju SN, Nimmi F, Sachin JS, Ramapurath SJ. Multifunctional hybrid nanoconstruct of zerovalent iron and carbon dots for magnetic resonance angiography and optical imaging: an in vivo study. Biomaterials. 2018;171:46.

39. Dresselhaus MS, Jorio A, Hofmann M, Dresselhaus G, Saito R. Perspectives on carbon nanotubes and graphene raman spectroscopy. Nano Lett. 2010;10:751.

40. Li YJ, Li W, Zhang HR, Dong RY, Li DN, Liu YL, Huang L, Lei BF. Biomimetic preparation of silicon quantum dots and its phytophysiology effect on cucumber seedling. J Mater Chem B. 2019;7(7):1107.

41. Song W, Liu YX, Fanady B, Han YF, Xie L, Chen ZY, Yu KB, Peng X, Zhang XL, Ge ZY. Ultra-flexible light-permeable organic solar cells for the herbal photosynthetic growth. Nano Energy. 2021;86: 106044.

42. Pan L, Sun S, Zhang L, Jiang K, Lin H. Near-infrared emissive carbon dots for two-photon fluorescence bioimaging. Nanoscale. 2016;8:17350.

43. Bojdys MJ, Müller JO, Antonietti M, Thomas A. Ionothermal synthesis of crystalline, condensed, graphitic carbon nitride. Chem Eur J. 2008;14:8177.

44. Qu D, Zheng M, Du P, Zhou Y, Zhang L, Li D, Tan H, Zhao Z, Xie Z, Sun Z. Highly luminescent S, N co-doped graphene quantum dots with broad visible absorption bands for visible light photocatalysts. Nanoscale. 2013;5:12272.

45. Liu J, Geng Y, Li D, Yao H, Huo Z, Li Y, Zhang K, Zhu S, Wei H, Xu W, Jiang J, Yang B. Deep red emissive carbonized polymer dots with unprecedented narrow full width at half maximum. Adv Mater. 2020;32:1906641.

46. Zhen S, van Iersel MW. Far-red light is needed for efficient photochemistry and photosynthesis. J Plant Physiol. 2017;209:115.

47. Park S, Steen CJ, Lyska D, Fischer AL, Endelman B, Iwai M, Niyogi KK, Fleming GR. Chlorophyll–carotenoid excitation energy transfer and charge transfer in *Nannochloropsis oceanica* for the regulation of photosynthesis. Proc Nat Acad Sci USA. 2019;116(9):3385.

48. Eyster C, Brown TE, Tanner HA, Hood SL. Manganese requirement with respect to growth, hill reaction and photosynthesis. Plant Physiol. 1958;33(4):235.

49. Ifuku K. The PsbP and PsbQ family proteins in the photosynthetic machinery of chloroplasts. Plant Physiol Biochem. 2014;81:108.

50. Jensen PE, Gilpin M, Knoetzel JR, Scheller HV. The PSI-K subunit of photosystem I is involved in the interaction between light-harvesting complex I and the photosystem I reaction center core. J Biol Chem. 2000;275(32):24701.

51. Shusuke K, Uno C, Ido K, Nishimura TS, Noguchi T, Ifuku K, Sato F. The PsbQ protein stabilizes the functional binding of the PsbP protein to photosystem II in higher plants. Biochim Biophys Acta. 2012;1817(8):1346.

52. Bricker TM, Roose JL, Fagerlund RD, Frankel LK, Eaton-Rye JJ. The extrinsic proteins of photosystem II. Biochim Biophys Acta. 2011;1817(1):121.

53. Sandhu D, Atkinson T, Noll A, Johnson C, Espinosa K, Boelter J, Abel S, Balpreet KD, Barta T, Singsaas E, Sepsenwol S, Goggi AS, Palmer RG. Soybean proteins GmTic110 and GmPsbP are crucial for chloroplast development and function. Plant Sci. 2016;252:76.

54. Yi X, Hargett SR, Frankel LK, Bricker TM. The PsbQ protein is required in *Arabidopsis* for photosystem II assembly/stability and photoautotrophy under low light conditions. J Biol Chem. 2006;281:26260.

55. Bricker TM, Frankel LK. Auxiliary functions of the PsbO, PsbP and PsbQ proteins of higher plant photosystem II: a critical analysis. J Photochem Photobiol B. 2011;104(1–2):165.

56. Komenda J, Nickelsen J, Tichy M, Prasin O, Eichacker LA, Nixon PJ. The cyanobacterial homologue of HCF136/YCF48 is a component of an early photosystem II assembly complex and is important for both the efficient assembly and repair of photosystem II in *Synechocystis* sp. PCC 6803. J Biol Chem. 2008;283(33):22390.

57. Shen G, Zhao J, Reimer SK, Antonkine ML, Cai Q, Weiland SM, Golbeck JH, Bryant DA. Assembly of photosystem I. I. Inactivation of the rubA gene encoding a membrane-associated rubredoxin in the cyanobacterium *Synechococcus* sp. PCC 7002 causes a loss of photosystem I activity. J Biol Chem. 2002;277(23):20343.

58. Lin S, Bhattacharya P, Rajapakse NC, Brune DE, Ke PC. Effects of quantum dots adsorption on algal photosynthesis. J Phys Chem C. 2009;113:10962.

59. Qian S, Qiao L, Xu W, Jiang K, Wang Y, Lin H. An inner filter effect-based near-infrared probe for the ultrasensitive detection of tetracyclines and quinolones. Talanta. 2019. https://doi.org/10.1016/j.talanta.2018.10.097.

Publisher's Note

Springer Nature remains neutral with regard to jurisdictional claims in published maps and institutional affiliations.